Fingerprints of Heavy-Element Nucleosynthesis in the Late-Time Lightcurves of Kilonovae

Meng-Ru Wu,[1,2,*] J. Barnes,[3,†] G. Martínez-Pinedo,[4,5,‡] and B. D. Metzger[3,§]
[1]*Institute of Physics, Academia Sinica, Taipei 11529, Taiwan*
[2]*Institute of Astronomy and Astrophysics, Academia Sinica, Taipei 10617, Taiwan*
[3]*Department of Physics and Columbia Astrophysics Laboratory, Columbia University, Pupin Hall, New York, New York 10027, USA*
[4]*GSI Helmholtzzentrum für Schwerionenforschung, Planckstraße 1, 64291 Darmstadt, Germany*
[5]*Institut für Kernphysik (Theoriezentrum), Technische Universität Darmstadt, Schlossgartenstraße 2, 64289 Darmstadt, Germany*

(Received 30 August 2018; revised manuscript received 15 November 2018; published 12 February 2019)

The kilonova emission observed following the binary neutron star merger event GW170817 provided the first direct evidence for the synthesis of heavy nuclei through the rapid neutron capture process (r process). The late-time transition in the spectral energy distribution to near-infrared wavelengths was interpreted as indicating the production of lanthanide nuclei, with atomic mass number $A \gtrsim 140$. However, compelling evidence for the presence of even heavier third-peak ($A \approx 195$) r-process elements (e.g., gold, platinum) or translead nuclei remains elusive. At early times (∼days) most of the r-process heating arises from a large statistical ensemble of β decays, which thermalize efficiently while the ejecta is still dense, generating a heating rate that is reasonably approximated by a single power law. However, at later times of weeks to months, the decay energy input can also possibly be dominated by a discrete number of α decays, ^{223}Ra (half-life $t_{1/2} = 11.43$ d), ^{225}Ac ($t_{1/2} = 10.0$ d, following the β decay of ^{225}Ra with $t_{1/2} = 14.9$ d), and the fissioning isotope ^{254}Cf ($t_{1/2} = 60.5$ d), which liberate more energy per decay and thermalize with greater efficiency than β-decay products. Late-time nebular observations of kilonovae which constrain the radioactive power provide the potential to identify signatures of these individual isotopes, thus confirming the production of heavy nuclei. In order to constrain the bolometric light to the required accuracy, multiepoch and wideband observations are required with sensitive instruments like the *James Webb* Space Telescope. In addition, by comparing the nuclear heating rate obtained with an abundance distribution that follows the solar r abundance pattern, to the bolometric lightcurve of AT2017gfo, we find that the yet-uncertain r abundance of ^{72}Ge plays a decisive role in powering the lightcurve, if one assumes that GW170817 has produced a full range of the solar r abundances down to mass number $A \sim 70$.

DOI: 10.1103/PhysRevLett.122.062701

Introduction.—The gravitational wave emission detected from the binary neutron star merger (NSM) GW170817 by Advanced LIGO [1] triggered a worldwide search for electromagnetic counterparts [2]. Within eleven hours of the coalescence, a fading blue thermal source, AT2017gfo, was discovered from the galaxy NGC 4993 [3,4]. The luminosity and evolution agreed with predictions for the light powered by the radioactive decay of heavy nuclei synthesized via the rapid neutron capture process (r process) in neutron-rich merger ejecta [5–8]. The presence of luminous visual wavelength ("blue") emission at early times was interpreted by most groups as arising from the fastest outer layers of the ejecta, which contained exclusively light r-process nuclei with a relatively low visual wavelength opacity [9–11] (see, however, Refs. [12,13]). The observed transition of the emission colors to the near-infrared confirmed predictions for the inner ejecta layers containing lanthanide elements, with atomic mass number $A \gtrsim 140$ [8,14,15]. The amount of the merger ejecta was estimated to be $M_{\rm ej} \approx 0.03$–$0.06\ M_\odot$ [12,13,16–19], with the bulk of which expanding at velocities of $v_{\rm ej} \approx 0.1$ c.

Although evidence exists for the presence of some lanthanides in the ejecta of GW170817, the detailed abundance pattern of the nuclei synthesized, and how it compares to those in the Solar System or metal-poor stars, remains less clear. This uncertainty arises partly because of incomplete atomic data for the relevant elements and ionization states, as well as the modeling of radiative transfer. Even with accurate modeling, most kilonova properties at early times ∼1–10 d, when the lightcurves are at their peaks, are insensitive to the presence of even heavier nuclei, such as the third-peak ($A \approx 195$) r-process elements (e.g., gold, platinum) and transuranic nuclei. Lanthanides are only produced in ejecta with low electron fraction, $Y_e \lesssim 0.25$ [9,20], while even smaller Y_e are needed to synthesize heavier isotopes. Whether the ejecta

TABLE I. Late-time kilonova models (see text for explanations).

Model	$Y_{e,c}$	ΔY_e	$A_{\rm peak}$	$M_{\rm ej}$ $(M_\odot)$	$v_{\rm ej}$ (c)	Nuclear masses
A	0.15	0.04	130 and 195	0.040	0.1	FRDM
B	0.25	0.04	80 and 130	0.040	0.1	FRDM
C	0.35	0.04	80	0.055	0.1	FRDM
D	0.45	0.04	60	0.030	0.1	FRDM
*A*1	0.15	0.04	130 and 195	0.020	0.1	DZ31

of GW170817 contained such low Y_e matter is presently unknown.

At times after ∼10 d, the ejecta becomes transparent, entering a "nebular" phase in analogy with those of supernovae, which are observed starting months after explosion. Although the uncertainties associated with the ejecta opacity become smaller as it dilutes, these are replaced by even larger uncertainties in calculating the nebular spectrum, due to the increasing importance of deviations from local thermodynamical equilibrium (see Ref. [21] for a review in the supernova context). Nevertheless, if one could measure the *bolometric* nebular emission, it should faithfully track the radioactive decay energy input.

Table I in the Supplemental Material (SM) [22] lists *all* 25 *r*-process isotopes with half-lives of 10–100 d that can contribute to late-time heating. Given the small number of isotopes, one might hope to detect the decay signatures of individual isotopes and their associated yields, in the way that the ^{56}Ni to ^{56}Co chain is observed in normal supernovae. As we shall show, these signatures could provide useful diagnoses of the range of heavy nuclei that are produced or even the elusive definitive proof that the heaviest nuclei in the universe are synthesized in NSM.

Late-time kilonova heating.—We first examine the late-time kilonova emission for a few ejecta models that contain distinct nuclear compositions, as listed in Table I. In each model, the total *r* process heating rate $\dot{Q}$ in the ejecta of total mass $M_{\rm ej}$ and average expansion velocity $v_{\rm ej}$ can be formulated as

$$\dot{Q}(t) = \sum_i f_i(t)\dot{q}_i(t)M_{\rm ej}. \quad (1)$$

It roughly equals the bolometric luminosity $L_{\rm bol}$ of the kilonova following its peak light, particularly at late time after the ejecta becomes optically thin. In Eq. (1), $\dot{q}_i(t)$ is the radioactive decay energy release rate per unit mass from a decay channel i, including β^--decay, β^+-decay or electron capture, α decay, and spontaneous fission. The thermalization efficiency $f_i(t)$ is defined by the ratio of the rate of the ejecta specific thermal energy increase to $\dot{q}_i(t)$ due to the thermalization of decay products. We assume that the material contains a Gaussian Y_e distribution, characterized by a central value $Y_{e,c}$ and a width ΔY_e. The corresponding $\dot{q}_i(t)$ is calculated using an *r*-process nuclear reaction network [23]. We adopt $f_i(t)$ of β^--decay products based on detailed particle thermalization simulations [24] while modeling those of dominating individual nuclei based on the work of Ref. [25]. These represent an important improvement when compared with recent works [26,27]. Detailed descriptions for the calculation of $\dot{q}_i(t)$ and $f_i(t)$ are given in the SM [22].

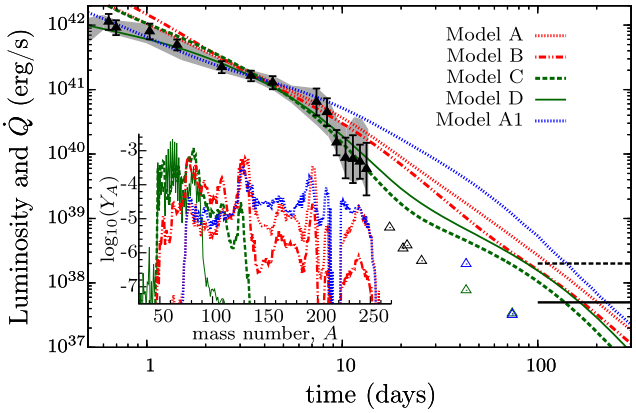

FIG. 1. $L_{\rm bol}$ of the kilonova associated with GW170817 from Ref. [28] (filled black triangles), including uncertainties (gray band) derived from the range of values given in Refs. [12,18,28]. Also shown are lower limits (empty triangles) on the late-time luminosity as inferred from the Ks band with VLT/HAWK-I [29] (black) and the 4.5 μm detections by the *Spitzer* Space Telescope from Ref. [30] (green) and Ref. [31] (blue). Colored lines show the ejecta heating rate $\dot{Q}(t)$ for different models listed in Table I. Their corresponding abundance distributions at $t = 1$ d are shown in the inset. The black solid (dashed) horizontal lines in the lower right corner represent the approximate observation limits of the NIR (MIR) instruments on the JWST for a merger at 100 Mpc.

For models *A*–*D*, we vary the ejecta Y_e distribution such that the produced peak and range of nuclei are largely distinct (see Table I and Fig. 1). Both models *A* and *B* with lower $Y_{e,c} = 0.15$ and 0.25 produce a wide range of nuclei across the two corresponding abundance peaks, $A_{\rm peak}$. On the other hand, models *C* and *D* with higher $Y_{e,c} = 0.35$ and 0.45 only produce a smaller range of nuclei around its $A_{\rm peak} = 80$ and 60.

Figure 1 shows the inferred $L_{\rm bol}$ of AT2017gfo and the heating rate $\dot{Q}(t)$ derived with models *A*–*D*. We vary the $M_{\rm ej}$ to match the normalization of the luminosity at ∼3–6 d. Note that as we focus on the bulk of the ejecta, we ignore the early time data which most likely originated from a fast-moving component with different composition and lower mass. Figure 1 shows clearly that the $L_{\rm bol}$ evolution in models that produce broad ranges of nuclei (*A* and *B*) starts to diverge from those with narrow ranges (*C* and *D*) at ∼7 d. In particular, the latter cases show a clear dip at ∼25 d. This difference originates from the number of nuclei that can decay on timescales greater than ∼days in each model. Both models *A* and *B* contain ∼10 nuclear species that can decay at late times between 10–100 d, such

that at any given time t one can find a nucleus with a commensurate β-decay lifetime $t_{1/2} \sim t$ contributing to the heating. This leads to a late-time power law behavior of $\dot{Q}(t)$ [6,32].

However, for models C and D which only produce nuclei around their $A_{\rm peak}$, the absence of nuclei with β-decay lifetimes in the range 10–50 d for $70 \leq A \leq 100$ (see Table I in the SM [22]) results in the observed light curve dips at ∼25 d. Note that in both cases, the resulting $\dot{Q}(t)$ are compatible with the $L_{\rm bol}(t)$ of AT2017gfo and cannot be ruled out by such a comparison alone (cf. Ref. [33] which assumed single-Y_e models). A well-measured $L_{\rm bol}(t)$ for future events covering 10–50 d can be used to infer the range of nuclei being produced in NSM. Therefore, it can provide complementary information about the nuclear composition, in addition to the inferred mass fraction of lanthanides and actinides derived from comparison to radiation transport models, due to their high opacities that results in the reddening of the spectra [8,15].

Models A–D use the same set of nuclear reactions. Previous studies show that the choice of theoretical nuclear physics inputs can affect significantly the kilonova light-curves [24,34] for low Y_e ejecta, as the r process involves extremely neutron-rich nuclei, whose key properties (masses, β decay half-lives, …) are not yet experimentally measured. Particularly important are the produced amount of translead nuclei that can undergo α decays or spontaneous fission at ≳days. As they release a relatively large amount of energy per decay and their decay products thermalize more efficiently than those of β decays, they can dominate the heating even in trace amounts. Here, we illustrate the nuclear physics impact using two sets of neutron-capture rates and their reverse photodissociation rates [35] which employ, respectively, nuclear masses from the finite-range droplet model (FRDM) [36] for models A–D and the Duflo-Zuker parametrization with 31 parameters (DZ31) [37] for model $A1$.

Model $A1$ produces translead nuclei with $220 \lesssim A \lesssim 230$ at the level of a few times 10^{-5}, a factor of ∼4–10 more than those by model A (see Fig. 1). Among those, four nuclei have α-decay half-lives between 1 and 100 d: ^{222}Rn ($t_{1/2} = 3.8$ d), ^{223}Ra ($t_{1/2} = 11.4$ d), ^{224}Ra ($t_{1/2} = 3.6$ d), and ^{225}Ac ($t_{1/2} = 10$ d, following the β decay of ^{225}Ra with $t_{1/2} = 14.9$ d). Their decay chains release a large amount of nuclear energy ∼30 MeV (see Table I in SM [22]), most of which goes into the kinetic energy of α particles, that thermalize more efficiently than β-decay products. These α decays can therefore compete with the β decays of many other nuclei at early time ($t \sim 2$–6 d) and dominate the heating rate at late times, despite the abundances. We find that the enhanced heating from α decays reduces the required $M_{\rm ej}$ to account for the AT2017gfo luminosity around 3-6 d by roughly a factor of 2 (see Table I). More importantly, it generates a broad "bumplike" feature at

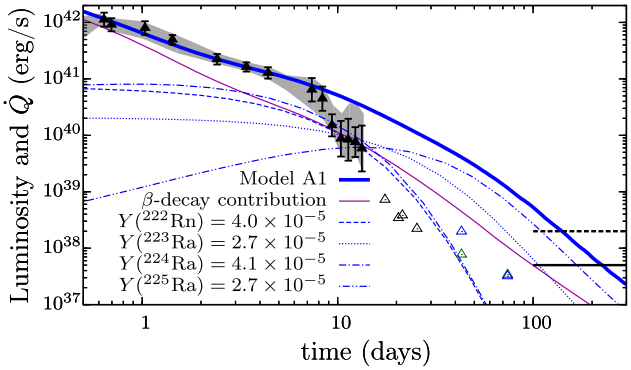

FIG. 2. Lightcurve for the model $A1$ (thick solid blue line) showing the dominating contributions to the total radioactive heating: beta decays (thin maroon line) and individual α decays (thin blue lines).

$t \approx 6$–200 d that is otherwise absent without actinide production. This feature is mostly driven by the $A = 225$ decay chain due to its effective long $t_{1/2}$ (see Fig. 2). As no other radioactive nuclei can release similar energy on this timescale, such a feature in future kilonova observations would uniquely point to the production of heavy nuclei up to the actinides in that mass range to the abundance level of a few times 10^{-5}. We also note that the steepening of the AT2017gfo $L_{\rm bol}$ at $t \sim 10$ d, places an upper limit of $\lesssim 10^{-5}$ for the total abundance of translead nuclei with $A =$ 222–225 This constraint may also be used to derive upper limits on the U and Th production in GW170817 and future NSM (see SM [22]).

Beyond the energy deposition from α decays, the potential importance of spontaneous fission heating was pointed out in Ref. [38] (also see Ref. [26] for a very recent work discussing the impact of ^{254}Cf fission on the light-curve). Similar to the α-decay nuclei, whether ^{254}Cf (or even heavier nuclei) can dominantly contribute to kilonova heating is subject to nuclear physics uncertainties. The production of α-decay nuclei is sensitive to the evolution of the $N = 162$ subshell closure for $Z \sim 80$ while the amount of ^{254}Cf (and neighboring nuclei) remaining at days is sensitive to the prediction of fission barriers that affect various fission rates of the progenitor nuclei [39]. Within our adopted nuclear input, we do not find a significant contribution of ^{254}Cf to the heating rate when averaged over a wide range of Y_e (see Fig. 1 for the low abundance of $A \gtrsim 250$). Instead, we explore such an effect by artificially including a fraction $Y(^{254}\mathrm{Cf}) = 2 \times 10^{-6}$ on top of the model A. Figure 3 shows that even such a tiny quantity of ^{254}Cf ($t_{1/2} = 60.5$ d) produces a lightcurve "bump" between 50–300 d. We find that this feature can be distinguished from that due to the late-time radioactive decay of ^{56}Co ($t_{1/2} = 77.24$ d), due to the very inefficient thermalization of the ^{56}Co decay products dominated by γ rays [40]. Note that a future identification of a bump feature

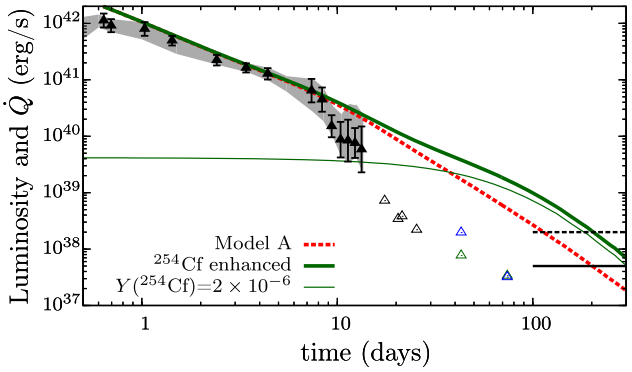

FIG. 3. The decay of ^{254}Cf could produce a late-time plateau in the lightcurve. This figure is the same as Fig. 1, but showing both the model A and a case with the ^{254}Cf abundance artificially enhanced.

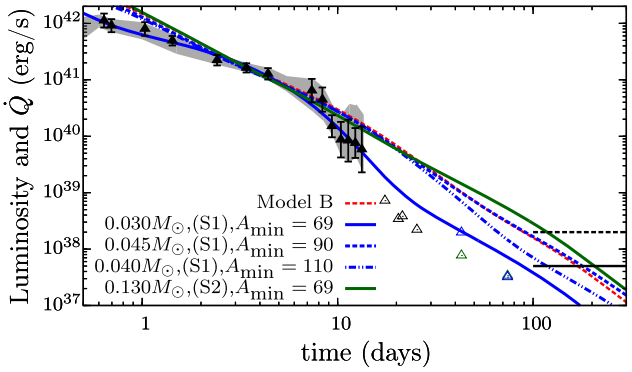

FIG. 4. The radioactive decay heating rate powered by the solar-r abundance distribution for nuclei between $A_{\rm min}$ and 205. We use two different abundance sets from [44,45]. See text for discussions.

that does not match the timescale by α decay or ^{254}Cf fission discussed above may suggest the production of yet-unknown long-lived superheavy nuclei.

Heating from solar r abundances.—One can ask whether the GW170817 kilonova is consistent with that expected for ejecta containing r-process nuclei with the solar abundance pattern. From detailed multiband lightcurve and spectral analyses, the inferred lanthanide mass fraction $X_{\rm lan}$ is $\sim 10^{-3}-10^{-2}$ [12,16,42]. Assuming that the GW170817 yield follows the solar proportions, such low $X_{\rm lan}$ requires the production of all r-process nuclei with additional contributions of trans-iron nuclei.

We approach this question from the viewpoint of comparing the luminosity of AT2017gfo to the radioactive heating rate $\dot{Q}(t)$, calculated under the assumption that the only heating contribution is from β decays and that the relative abundances of the unstable nuclei follow exactly the solar r abundances ratios between some minimum mass number $A_{\rm min}$ and $A_{\rm max}=205$ [43]. We employ two sets of the solar r abundances from Ref. [44] (S1) and Ref. [45] (S2).

Figure 4 shows that with $A_{\rm min}=90$ or 110, the resulting $\dot{Q}$ roughly matches $L_{\rm bol}$ of AT2017gfo for $M_{\rm ej}\simeq 0.04\ M_\odot$. In fact, they closely resemble the model B prediction and both S1 and S2 give consistent results. However, such abundance patterns would have $X_{\rm lan}\gtrsim 0.1$, which is inconsistent with spectral modeling of AT2017gfo.

If we instead consider that GW170817 produced the solar r-process pattern down to $A_{\rm min}=69$ (in order to reduce $X_{\rm lan}$ to values consistent with spectral modeling), for the S1 abundances the resulting $\dot{Q}$ can also be consistent with the $L_{\rm bol}$ of AT2017gfo. This model, however, diverges from the $A_{\rm min}=90$ or 110 light curves beyond 10 d, a difference testable in future events. On the other hand, adopting the S2 abundances requires an uncomfortably large $M_{\rm ej}\gtrsim 0.13\ M_\odot$ to match the observed $L_{\rm bol}$. This large difference arises because the abundance of ^{72}Ge in S1 is similar to its neighboring nuclei, ^{70}Zn and ^{74}Ge, while for S2 the ^{72}Ge abundance is zero. The only nucleus between $A=69$–90 that contributes significantly to the heating is the decay sequence, ^{72}Zn ($t_{1/2}=1.94$ d) to ^{72}Ga ($t_{1/2}=0.59$ d) to ^{72}Ge, that releases a net energy $\sim$3.5 MeV per decay. The β-decay contribution of ^{72}Zn in S1 thus gives rise to the bump feature at 2–5 d that is lacking for the S2 set. By artificially varying the $A=72$ mass fraction, we find that at least $\gtrsim$20% of its S1 abundance is needed to match the GW170817 light curve for $M_{\rm ej}\lesssim 0.05\ M_\odot$ (see SM [22] for details).

Taken together, we conclude that GW170817 may have produced a solarlike r-process yield down to $A\sim 70$, if the solar r-process contribution to the ^{72}Ge abundance is larger than $\sim$20% of the value given by S1. However, if the solar r abundance of ^{72}Ge abundance turns out to be much smaller than that of ^{70}Zn and ^{74}Ge, then either a substantial additional heating from $A<69$ isotopes (e.g., ^{66}Ni, see [27]) would be required to make GW170817 consistent with the solar abundances, or one would require enhanced lighter nuclei yields in $A\sim 90$–130 relative to the heavier nuclei beyond the second peak, when compared to the solar r abundances, to give $X_{\rm lan}\lesssim 0.01$. We note, however, that the correlation of the abundances of Ge and Fe in metal-poor stars and the noncorrelation of Ge and Eu [46] hints that NSM are unlikely to produce the entire solar r abundances down to $A\approx 70$.

Discussion.—Our results demonstrate how late-time bolometric kilonova lightcurves can provide an important diagnostic of the nuclear composition of the NSM ejecta. Recently, Refs. [30,31] reported detections of GW170817 at 43 and 74 d postmerger in the wavelength band centered at 4.5 μm using the *Spitzer* Space Telescope; the 3.6 μm band was also observed, resulting in nondetections. Interpreted as blackbody emission, the observed colors indicate that the ejecta had cooled by these late times to temperatures $\lesssim$1200 K. Unfortunately, the ejecta during the nebular phase radiate through discrete spectral lines

rather than as a blackbody, and so translating these observations into a bolometric luminosity is challenging. Making the very conservative assumption of counting only the luminosity in the detected band, these lower limits (shown as open triangles in Figs. 1–4) are not constraining in most of the cases. The only exception is the scenario with heating powered by solar r abundances with $A_{\rm min} = 69$ with the abundance set S1, for which the late-time lightcurve is in tension with the data at 43 d of Ref. [31].

Observations of future merger events by, e.g., the *James Webb* Space Telescope (JWST) could be more promising [30]. For a merger at 100 Mpc, the NIRcam instrument on JWST could detect luminosities in the $\approx$0.6–4 μm band down to $L_{\rm NIR} \approx 5 \times 10^{37}$ erg s^{-1} (for a $S/N = 10$ detection given a 10^4 s integration), sufficient to distinguish various models shown in, e.g., Fig. 1 out to timescales of months. The midinfrared instrument (MIRI) sensitive in the 5–14 μm band, could constrain the luminosity to $L_{\rm MIR} \approx 2 \times 10^{38}$ erg s^{-1}. We emphasize that well time-sampled observations, which cover as wide in optical and infrared frequency range as possible, will be necessary to constrain the bolometric lightcurve evolution with sufficient precision to distinguish the nuclear physics features discussed here.

A number of uncertainties could affect future nebular measurements, which requires additional theoretical modeling. The ejecta may not radiate the radioactive heating it receives with complete efficiency. Empirically, the lightcurves of Type I*a* supernovae faithfully track the radioactive decay input up to several years [47]. However, at later times the situation is less clear; nonthermally excited ions might absorb a large fraction of the radioactive energy, but due to the low density the rate of recombination could be slow and the energy released much later than injection ("freeze-out"; [48]). Freeze-out sets in on timescales of years in supernovae (see Fig. 7 of Ref. [47]), which, if occurring at the same density in a NSM, would translate into an even earlier timescale of weeks to months due to their lower ejecta mass and faster expansion speeds.

The authors acknowledge useful discussions with Andrei Andreyev, Ben Gibson, Karlheinz Langanke, Karl-Heinz Schmidt and Friedrich-Karl Thielemann, as well as anonymous referees for their helpful comments. M.-R. W. acknowledges support from the Ministry of Science and Technology, Taiwan under Grant No. 107-2119-M-001-038. J. B. is supported by the National Aeronautics and Space Administration (NASA) through the Einstein Fellowship Program, Grant No. PF7-180162. G. M.-P. is partly supported by the Deutsche Forschungsgemeinschaft (DFG, German Research Foundation)–Projektnummer 279384907–SFB 1245. B. D. M. acknowledges support from NASA through the Astrophysics Theory Program, Grant No. NNX16AB30G. Computations were partly performed on the LOEWE-CSC computer managed by Center for Scientific Computing of the Goethe University Frankfurt. We thank the ExtreMe Matter Institute EMMI at GSI, Darmstadt, for support in the framework of the EMMI Rapid Reaction Task Force "The physics of neutron star mergers at GSI/FAIR" during which this work has been initiated.

*mwu@gate.sinica.edu.tw
†jlb2331@columbia.edu
NASA Einstein Fellow.
‡g.martinez@gsi.de
§bdm2129@columbia.edu

[1] B. P. Abbott *et al.* (LIGO Scientific and Virgo Collaborations), Phys. Rev. Lett. **119**, 161101 (2017).
[2] B. P. Abbott *et al.*, Astrophys. J. **848**, L12 (2017).
[3] D. A. Coulter *et al.*, Science **358**, 1556 (2017).
[4] M. Soares-Santos *et al.* (Dark Energy Camera GW-EM Collaboration), Astrophys. J. **848**, L16 (2017).
[5] L. Li and B. Paczyński, Astrophys. J. **507**, L59 (1998).
[6] B. D. Metzger, G. Martínez-Pinedo, S. Darbha, E. Quataert, A. Arcones, D. Kasen, R. Thomas, P. Nugent, I. V. Panov, and N. T. Zinner, Mon. Not. R. Astron. Soc. **406**, 2650 (2010).
[7] L. F. Roberts, D. Kasen, W. H. Lee, and E. Ramirez-Ruiz, Astrophys. J. Lett. **736**, L21 (2011).
[8] J. Barnes and D. Kasen, Astrophys. J. **775**, 18 (2013).
[9] B. D. Metzger and R. Fernández, Mon. Not. R. Astron. Soc. **441**, 3444 (2014).
[10] M. Nicholl *et al.*, Astrophys. J. **848**, L18 (2017).
[11] M. R. Drout *et al.*, Science **358**, 1570 (2017).
[12] E. Waxman, E. Ofek, D. Kushnir, and A. Gal-Yam, Mon. Not. R. Astron. Soc. **481**, 3423 (2018).
[13] K. Kawaguchi, M. Shibata, and M. Tanaka, Astrophys. J. **865**, L21 (2018).
[14] D. Kasen, N. R. Badnell, and J. Barnes, Astrophys. J. **774**, 25 (2013).
[15] M. Tanaka and K. Hotokezaka, Astrophys. J. **775**, 113 (2013).
[16] D. Kasen, B. Metzger, J. Barnes, E. Quataert, and E. Ramirez-Ruiz, Nature (London) **551**, 80 (2017).
[17] M. M. Kasliwal *et al.*, Science **358**, 1559 (2017).
[18] P. S. Cowperthwaite *et al.*, Astrophys. J. **848**, L17 (2017).
[19] V. A. Villar, J. Guillochon, E. Berger, B. D. Metzger, P. S. Cowperthwaite, M. Nicholl, K. D. Alexander, P. K. Blanchard, R. Chornock, T. Eftekhari, W. Fong, R. Margutti, and P. K. G. Williams, Astrophys. J. **851**, L21 (2017).
[20] J. Lippuner and L. F. Roberts, Astrophys. J. **815**, 82 (2015).
[21] A. Jerkstrand, Spectra of Supernovae in the nebular phase, in *Handbook of Supernovae*, edited by A. W. Alsabti and P. Murdin (Springer International Publishing, Cham, 2017), pp. 795–842.
[22] See Supplemental Material at http://link.aps.org/supplemental/10.1103/PhysRevLett.122.062701 for detail information.
[23] M.-R. Wu, R. Fernández, G. Martínez-Pinedo, and B. D. Metzger, Mon. Not. R. Astron. Soc. **463**, 2323 (2016).
[24] J. Barnes, D. Kasen, M.-R. Wu, and G. Martínez-Pinedo, Astrophys. J. **829**, 110 (2016).
[25] D. Kasen and J. Barnes, arXiv:1807.03319.

[26] Y. Zhu *et al.*, Astrophys. J. Lett. **863**, L23 (2018).
[27] S. Wanajo, Astrophys. J. **868**, 65 (2018).
[28] S. J. Smartt *et al.*, Nature (London) **551**, 75 (2017).
[29] N. R. Tanvir *et al.*, Astrophys. J. **848**, L27 (2017).
[30] V. A. Villar *et al.*, Astrophys. J. **862**, L11 (2018).
[31] M. M. Kasliwal *et al.*, arXiv:1812.08708.
[32] O. Korobkin, S. Rosswog, A. Arcones, and C. Winteler, Mon. Not. R. Astron. Soc. **426**, 1940 (2012).
[33] S. Rosswog, J. Sollerman, U. Feindt, A. Goobar, O. Korobkin, C. Fremling, and M. Kasliwal, Astron. Astrophys. **615**, A132 (2018).
[34] S. Rosswog, U. Feindt, O. Korobkin, M. R. Wu, J. Sollerman, A. Goobar, and G. Martinez-Pinedo, Classical Quantum Gravity **34**, 104001 (2017).
[35] J. J. Mendoza-Temis, M.-R. Wu, K. Langanke, G. Martínez-Pinedo, A. Bauswein, and H.-T. Janka, Phys. Rev. C **92**, 055805 (2015).
[36] P. Moller, J. R. Nix, W. D. Myers, and W. J. Swiatecki, Atom. Data Nucl. Data Tabl. **59**, 185 (1995).
[37] J. Duflo and A. P. Zuker, Phys. Rev. C **52**, R23 (1995).
[38] S. Wanajo, Y. Sekiguchi, N. Nishimura, K. Kiuchi, K. Kyutoku, and M. Shibata, Astrophys. J. **789**, L39 (2014).
[39] N. Vassh *et al.*, arXiv:1810.08133.
[40] It is interesting to note that ^{254}Cf was proposed to power the lightcurves of type Ia supernovae [41].
[41] G. R. Burbidge, F. Hoyle, E. M. Burbidge, R. F. Christy, and W. A. Fowler, Phys. Rev. **103**, 1145 (1956).
[42] M. Tanaka *et al.*, Publ. Astron. Soc. Jpn. **69**, 102 (2017).
[43] M. Tanaka, K. Hotokezaka, K. Kyutoku, S. Wanajo, K. Kiuchi, Y. Sekiguchi, and M. Shibata, Astrophys. J. **780**, 31 (2014).
[44] C. Sneden, J. J. Cowan, and R. Gallino, Annu. Rev. Astron. Astrophys. **46**, 241 (2008).
[45] S. Goriely, Astron. Astrophys. **342**, 881 (1999).
[46] J. J. Cowan, C. Sneden, T. C. Beers, J. E. Lawler, J. Simmerer, J. W. Truran, F. Primas, J. Collier, and S. Burles, Astrophys. J. **627**, 238 (2005).
[47] W. E. Kerzendorf, C. McCully, S. Taubenberger, A. Jerkstrand, I. Seitenzahl, A. J. Ruiter, J. Spyromilio, K. S. Long, and C. Fransson, Mon. Not. R. Astron. Soc. **472**, 2534 (2017).
[48] C. Fransson and C. Kozma, Astrophys. J. **408**, L25 (1993); C. Fransson and A. Jerkstrand, Astrophys. J. **814**, L2 (2015).